Supplementary Information

Fast, Efficient and Clean Adsorption of Bisphenol-A Using Renewable Mesoporous Silica Nanoparticles from Sugarcane Waste Ash

Suzimara Rovani[*a], Jonnatan J. Santos[b], Sabine N. Guilhen[a], Paola Corio[b] and Denise A. Fungaro[a]

[a] Instituto de Pesquisas Energéticas e Nucleares, IPEN-CNEN/SP - Av. Prof. Lineu Prestes, 2242 - Cidade Universitária - CEP 05508-000, São Paulo - SP - Brazil. *E-mail: suzirovani@gmail.com

[b] Instituto de Química, Universidade de São Paulo - Av. Prof. Lineu Prestes, 748 - Cidade Universitária - P.O. Box 26077 - CEP 05508-000, São Paulo, SP, Brazil.

Kinetic Adsorption Models

Kinetic adsorption models used in this publication were pseudo-first order[1, 2] (Eq. S1) and pseudo-second order[3-5] (Eq. S2).

$$q_t = q_e.\left(1 - e^{(-k_1 t)}\right) \qquad \text{(Eq. S1)}$$

$$q_t = \frac{k_2 \, . \, q_e^2 \; t}{1 + k_2 \, . \, q_e \, . \, t} \qquad \text{(Eq. S2)}$$

where in the Eq. S1, q_t is the amount of adsorbate adsorbed at time t (mg g^{-1}), q_e is the equilibrium adsorption capacity (mg g^{-1}), k_1 is the pseudo-first-order rate constant (h^{-1}), and t is the contact time (h). Eq. S2, k_2 is the pseudo-second-order rate constant (g mg^{-1} h^{-1}).[6-8]

Validation of Adsorption Kinetics

Chi-square (Eq. S3) was used to validate the kinetics model.[9]

$$X^2 = \sum_{i=1}^{n} \frac{\left(q_{exp} - q_{cal}\right)2}{q_{cal}} \qquad \text{(Eq. S3)}$$

q_{exp} and q_{cal} are experimentally determined quantity adsorbed at equilibrium and calculated quantity adsorbed at equilibrium respectively.

Other Kinetic Adsorption Models

Elovich model

The nonlinear form of the Elovich kinetic model is expressed by the Eq. S4.[9]

$$q_t = \beta . \ln(\alpha . \beta . t) \qquad \text{(Eq. S4)}$$

q_t is the quantity of adsorbate adsorbed at time t (mg g^{-1}), α is a constant related to chemisorption rate and β is a constant which depicts the extent of surface coverage.

Fractional power kinetic model

The nonlinear form of the Fractional power kinetic model is expressed by the Eq. S5.[9]

$$q_t = \mathrm{K}.\mathrm{t}^{\mathrm{v}} \quad \text{(Eq. S5)}$$

q_t is the quantity of adsorbate adsorbed at time t (mg g^{-1}), K is constant, v is constant that is usually less than unity if adsorption kinetic data fit well into the power function model.

Equilibrium Adsorption Models

Equilibrium adsorption models utilized were Langmuir[10] (Eq. S6); Freundlich[11] (Eq. S7) and Liu[8] (Eq. S8).

$$q_e = \frac{Q_{max}\,.\,K_L\,.\,C_e}{1 + K_L\,.\,C_e} \quad \text{(Eq. S6)}$$

q_e is the amount of adsorbate adsorbed at the equilibrium (mg g^{-1}), C_e is the adsorbate concentration at the equilibrium, i.e., C_e is the adsorbate concentration residual on solution (mg L^{-1}), K_L is the Langmuir equilibrium constant (L mg^{-1}), and Q_{max} is the maximum adsorption capacity of the adsorbent (mg g^{-1}).[8]

$$q_e = K_F\,.\,C_e^{\frac{1}{n_F}} \quad \text{(Eq. S7)}$$

K_F is the Freundlich equilibrium constant (mg g^{-1}(mg $L^{-1})^{-1/nF}$), n_F is the Freundlich exponent (dimensionless) and C_e is the adsorbate concentration residual on solution (mg L^{-1}).[8]

$$q_e = \frac{Q_{max}.\,(K_g\,.\,C_e)^{n_L}}{1 + (K_g\,.\,C_e)^{n_L}} \quad \text{(Eq. S8)}$$

K_g is the Liu equilibrium constant (L mg^{-1}); n_L is dimensionless exponent of the Liu equation; Q_{max} is the maximum adsorption capacity of the adsorbent (mg g^{-1}), C_e is the adsorbate concentration residual on solution (mg L^{-1}) and n_L could assume any positive value.[8]

TEM images

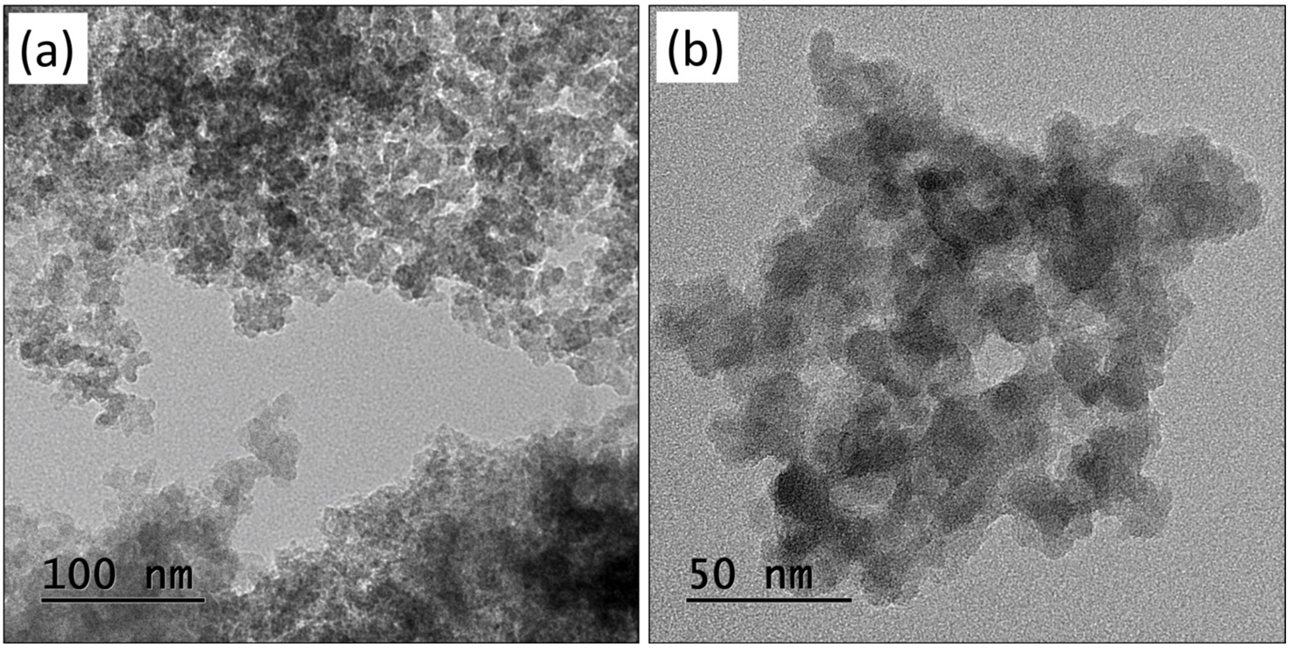

Fig. S1 TEM images of mesoporous silica nanoparticles (MSN-CTAB) with two different magnifications.

Study of the Effect of pH

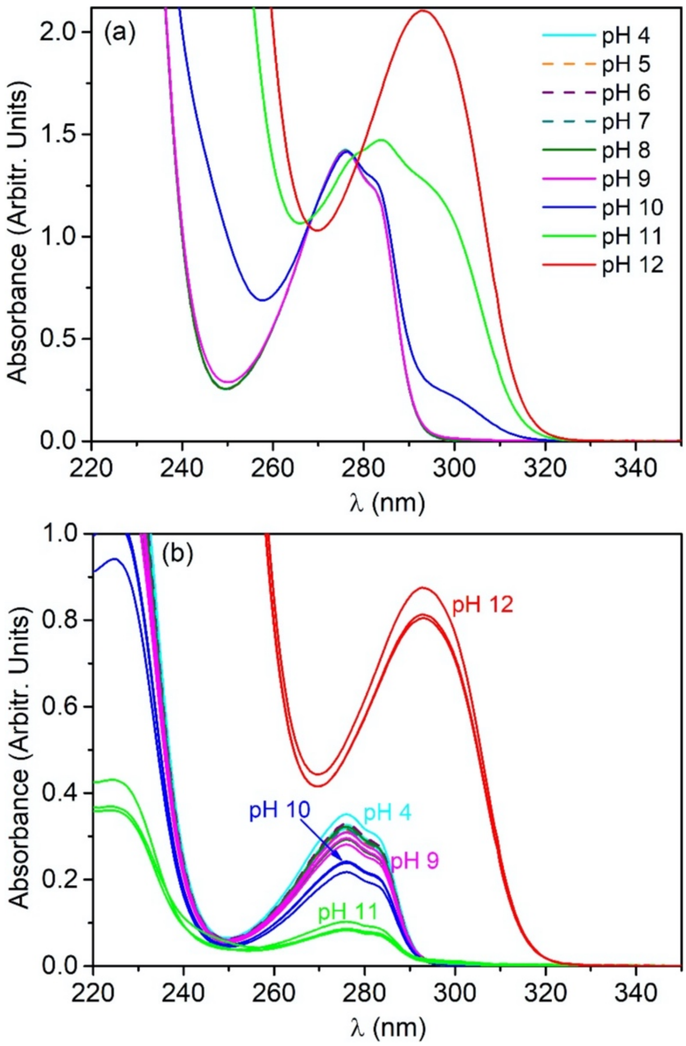

Fig. S2 UV spectra before BPA adsorption (a) initial solution 100 mg L^{-1} at different pH values from 4 to 12; and after 2h of BPA adsorption for 190 rpm at 25 °C (b) pH values from 4 to 12. Samples in triplicate.

In the bisphenol-A solutions at pH 10, 11, and 12 (Fig. S2a). The shift was due to a change in pH in which a higher pH resulted in deprotonation of the compounds which allowed increased conjugation. Conjugation lowers the energy of the bonds in the molecule resulting in a redshift of the λ_{max}. Therefore, the pH of the samples for UV-Vis analysis needed to be regulated to maintain the wavelength of maximum absorption for quantification.[12]

Table S1. Effect of the initial pH on the adsorption capacity of BPA. Conditions: 25 °C, initial concentration 100 mg L^{-1}, contact time 2 h and adsorbent mass 1.0 g L^{-1}.

Initial pH	Final pH	q experimental (mg g^{-1})
(4) 4.1	4.4	75.74 ± 0.8862
(5) 4.9	5.1	76.88 ± 1.103
(6) 5.9	5.4	75.98 ± 0.3586
(7) 7.0	5.6	78.46 ± 0.7024
(8) 8.0	5.4	77.93 ± 1.466
(9) 9.1	5.6	78.54 ± 0.1994
(10) 9.9	6.7	83.28 ± 0.4766
(11) 10.9	**9.3**	**91.98 ± 1.585**
(12) 11.9	11.6	59.26 ± 0.7943

BPA Calibration Curve

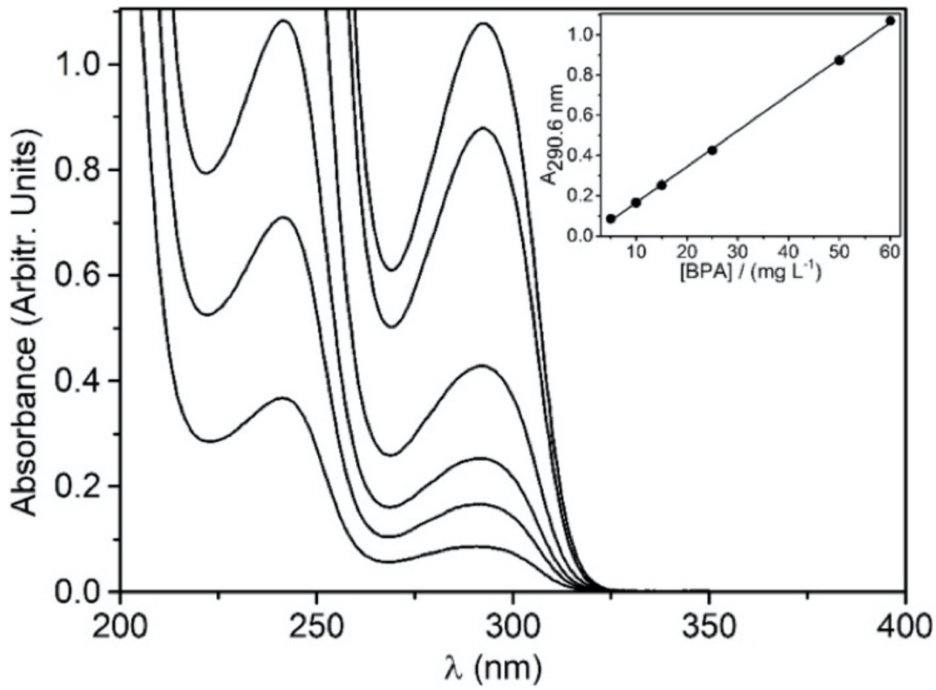

Fig. S3 UV spectra of the BPA-containing solution at pH 11 at concentrations ranging from 5.00 to 60.0 mg L^{-1}. Inserted graph: BPA analytical curve at pH 11.

Kinetic Study

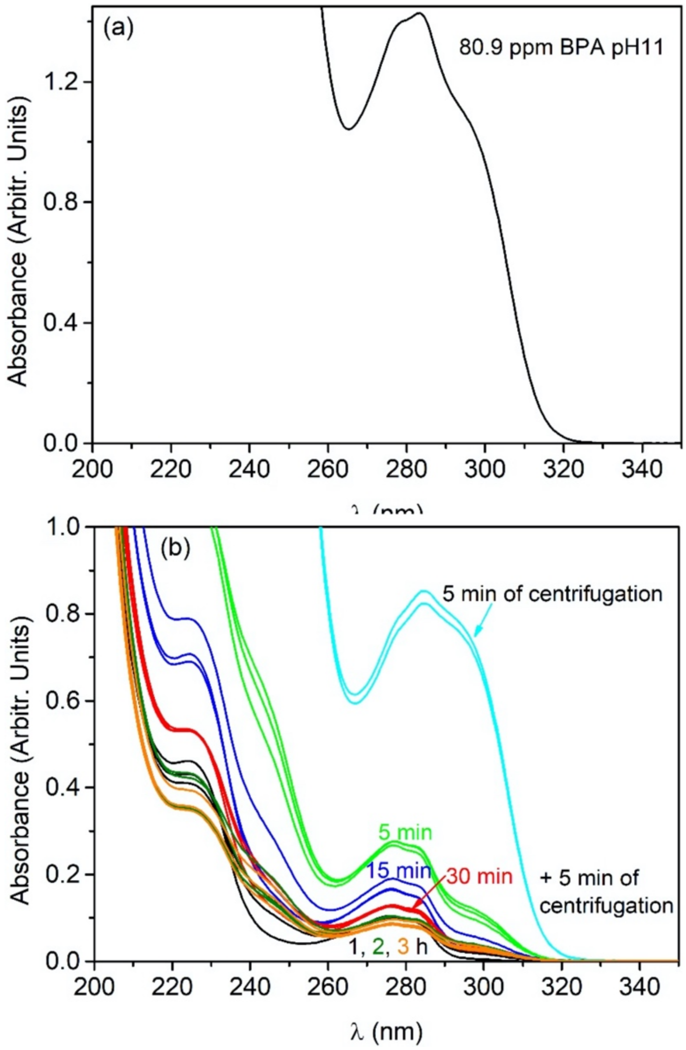

Fig. S4 UV spectra before BPA adsorption (a) initial solution 80.9 mg L^{-1} at pH 11; and after BPA adsorption at 25 °C (b) 5 min of centrifugation, 5 min to 3 h + 5 min of centrifugation. Samples in triplicate.

Table S2. Effect of the contact time on the adsorption capacity of BPA.

Time (minutes)	Initial pH	Final pH	q_t experimental (mg g^{-1})
(5 min of centrifugation)	11	10.5	33.11 $\pm$ 1.149
5 + (5 min of centrifugation)	11	9.8	66.49 $\pm$ 0.4466
15 + (5 min of centrifugation)	11	9.9	72.10 $\pm$ 0.8751
30 + (5 min of centrifugation)	11	9.8	74.24 $\pm$ 0.2475
60 + (5 min of centrifugation)	**11**	**9.5**	**75.59 $\pm$ 0.1170**
90 + (5 min of centrifugation)	11	9.9	75.20 $\pm$ 0.2636
120 + (5 min of centrifugation)	11	9.7	75.51 $\pm$ 0.4865
180 + (5 min of centrifugation)	11	9.7	75.86 $\pm$ 0.3614

Table S3. Kinetic parameters of BPA adsorption on MSN-CTAB.

Pseudo-first-order	**Calculated**	**Experimental**
k_f (min^{-1})	0.1506 $\pm$ 0.0172	-
q_e (mg g^{-1})	75.79 $\pm$ 1.696	75.59 $\pm$ 0.1170
$R^2_{ajd.}$	0.9784	-
X^2	0.000529	-
Pseudo-second-order	**Calculated**	**Experimental**
k_s (g mg^{-1} min^{-1})	3.006 x 10^{-3} $\pm$ 0.0196	-
q_e (mg g^{-1})	80.51 $\pm$ 3.443	75.59 $\pm$ 0.1170
$R^2_{ajd.}$	0.9470	-
X^2	0.3202	-

Pseudo-first-order model:

Nonlinear Curve Fit (BoxLucas1) (05/05/2020 09:02:05)

Parameters

		Value	Standard Error
qt	a	75.79348	1.69616
	b	0.15062	0.01721

Reduced Chi-sqr = 15.3064025454
COD(R^2) = 0.98111454193452
Iterations Performed = 1
Total Iterations in Session = 1
Fit converged. Chi-Sqr tolerance value of 1E-9 was reached.

Statistics

	qt
Number of Points	9
Degrees of Freedom	7
Reduced Chi-Sqr	15.3064
Residual Sum of Squares	107.14482
Adj. R-Square	0.97842
Fit Status	Succeeded(100)

Pseudo-second-order model:

Nonlinear Curve Fit (RectHyperbola) (05/05/2020 09:03:29)

Parameters

		Value	Standard Error
qt	a	80.51322	3.4428
	b	0.24205	0.06781

Reduced Chi-sqr = 37.5921857066
COD(R^2) = 0.95361773319078
Iterations Performed = 1
Total Iterations in Session = 1
Fit converged. Chi-Sqr tolerance value of 1E-9 was reached.

Statistics

	qt
Number of Points	9
Degrees of Freedom	7
Reduced Chi-Sqr	37.59219
Residual Sum of Squares	263.1453
Adj. R-Square	0.94699
Fit Status	Succeeded(100)

Other kinetic models:

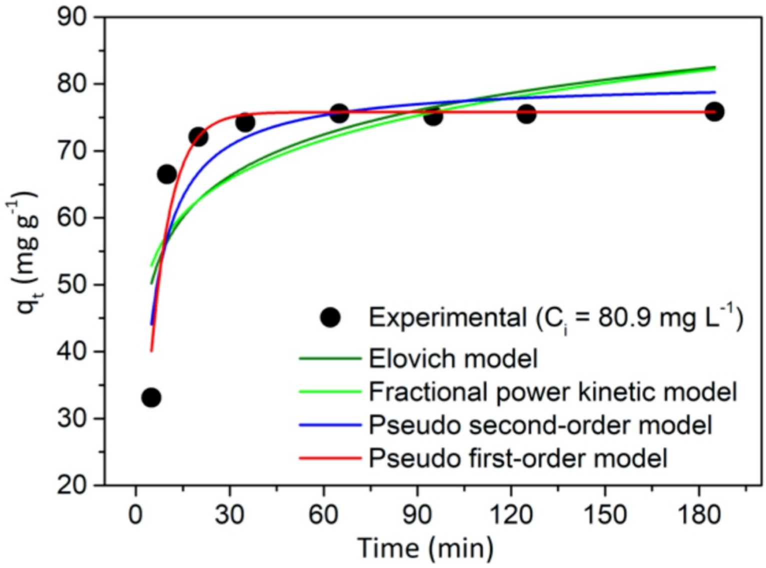

Fig. S5 Models kinetics plot for the removal of BPA by MSN-CTAB. (adsorbent mass 1.0 g L^{-1}).

Table S4. Kinetic parameters of BPA adsorption on MSN-CTAB.

Pseudo-first-order	**Calculated**
k_f (min^{-1})	0.1506 ± 0.0185
q_e (mg g^{-1})	75.79 ± 1.832
$R^2_{ajd.}$	0.9167
Pseudo-second-order	**Calculated**
k_s (g mg^{-1} min^{-1})	3 x 10^{-3} ± 0.0010
q_e (mg g^{-1})	80.51 ± 3.717
$R^2_{ajd.}$	0.7955
Elovich	**Calculated**
α (mg g^{-1} min^{-1})	6.144 ± 17.75
β (mg g^{-1})	8.942 ± 2.948
$R^2_{ajd.}$	0.5396
Fractional power	**Calculated**
V (min$^{-1)}$	0.1224 ± 0.0489
K (mg g^{-1})	43.38 ± 8.777
$R^2_{ajd.}$	0.4784

Pseudo-first-order model:

Nonlinear Curve Fit (BoxLucas1) (25/06/2020 13:40:47)

Parameters

		Value	Standard Error
qt	a	75.79348	1.83207
	b	0.15062	0.01859

Reduced Chi-sqr = 17.8574696362
COD(R^2) = 0.92862152884418
Iterations Performed = 1
Total Iterations in Session = 1
Fit converged. Chi-Sqr tolerance value of 1E-9 was reached.

Statistics

	qt
Number of Points	8
Degrees of Freedom	6
Reduced Chi-Sqr	17.85747
Residual Sum of Squares	107.14482
Adj. R-Square	0.91673
Fit Status	Succeeded(100)

Pseudo-second-order model:

Nonlinear Curve Fit (pseudo2ordem (User)) (25/06/2020 13:34:03)

Parameters

		Value	Standard Error
qt	k	0.00301	0.00101
	qe	80.51307	3.71701

Reduced Chi-sqr = 43.8575500057
COD(R^2) = 0.82469605538643
Iterations Performed = 1
Total Iterations in Session = 1
Fit converged. Chi-Sqr tolerance value of 1E-9 was reached.

Statistics

	qt
Number of Points	8
Degrees of Freedom	6
Reduced Chi-Sqr	43.85755
Residual Sum of Squares	263.1453
Adj. R-Square	0.79548
Fit Status	Succeeded(100)

Elovich model:

Nonlinear Curve Fit (Elovich (User)) (24/06/2020 16:48:43)

Parameters

		Value	Standard Error
qt	a	6.14403	17.75619
	b	8.94257	2.94779

Reduced Chi-sqr = 98.7352817162
COD(R^2) = 0.60534310842408
Iterations Performed = 1
Total Iterations in Session = 1
Fit converged. Chi-Sqr tolerance value of 1E-9 was reached.

Statistics

	qt
Number of Points	8
Degrees of Freedom	6
Reduced Chi-Sqr	98.73528
Residual Sum of Squares	592.41169
Adj. R-Square	0.53957
Fit Status	Succeeded(100)

Fractional power kinetic model:

Nonlinear Curve Fit (FractionalPower (User)) (24/06/2020 16:58:44)

Parameters

		Value	Standard Error
qt	K	43.38569	8.77778
	v	0.12242	0.04894

Reduced Chi-sqr = 111.854711937
COD(R^2) = 0.55290315524766
Iterations Performed = 1
Total Iterations in Session = 1
Fit converged. Chi-Sqr tolerance value of 1E-9 was reached.

Statistics

	qt
Number of Points	8
Degrees of Freedom	6
Reduced Chi-Sqr	111.85471
Residual Sum of Squares	671.12827
Adj. R-Square	0.47839
Fit Status	Succeeded(100)

Thermogravimetric Analysis

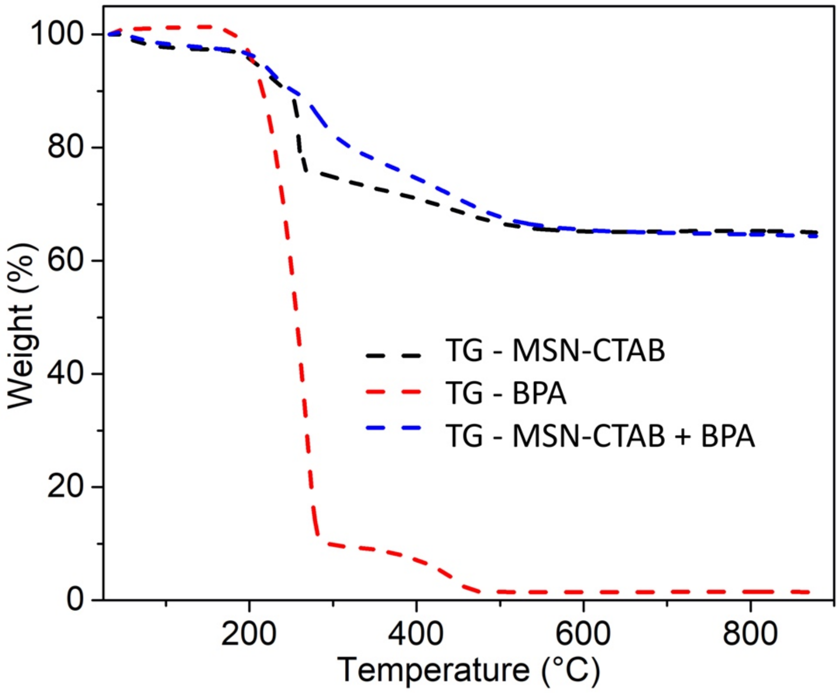

Fig. S6 TG curves of MSN-CTAB, BPA and MSN-CTAB + BPA.

Table S5. Thermogravimetric analysis of MSN-CTAB, BPA and MSN-CTAB after BPA adsorption.

Samples	1st wt. loss (%)	2nd wt. loss (%)	3rd wt. loss (%)	4th wt. loss (%)	Residue (%)
MSN-CTAB	(25-120 °C) 2.05	(120-235 °C) 7.85	(235-274 °C) 14.22	(274-550 °C) 10.54	65.34
BPA	(25-155 °C) 2.53	(155-300 °C) 87.87		(300-470 °C) 8.60	1.00
MSN-CTAB + BPA	(25-120 °C) 2.57	(120-250 °C) 8.71	(250-337 °C) 9.97	(337-550 °C) 13.19	65.56

Isotherm Study

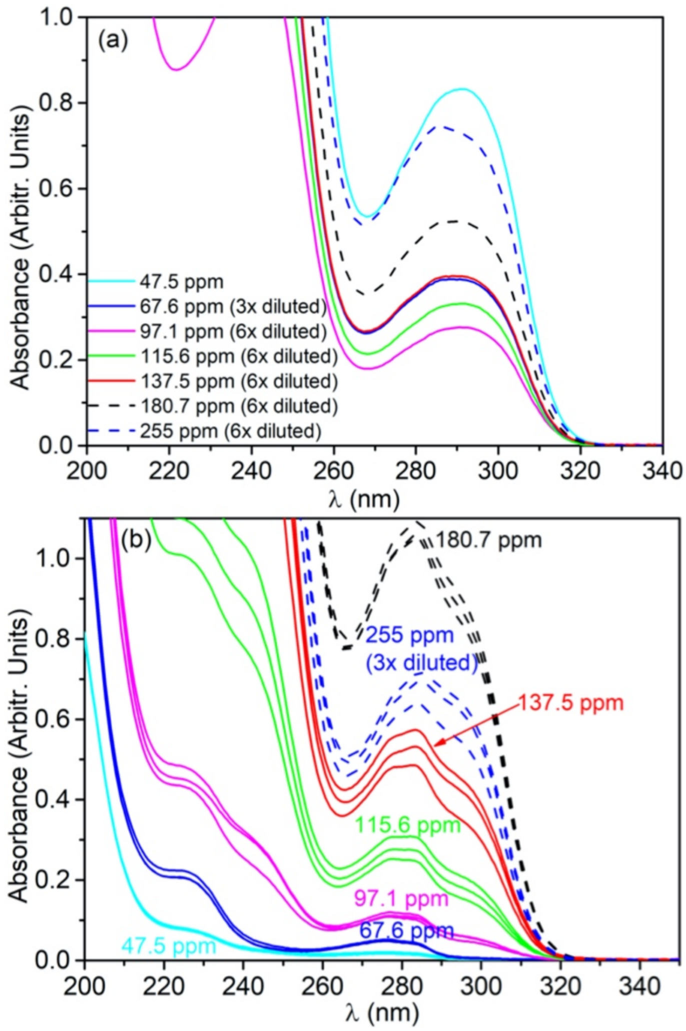

Fig. S7 UV spectra before BPA adsorption (a) initial solutions at pH 11 and concentrations from 47.5 to 255 mg L^{-1}; and after BPA adsorption at equilibrium time 1 h (b) 25°C isotherm. Samples in triplicate.

Table S6. Effect of the initial concentration on the adsorption capacity of BPA in pH 11.

Initial Concentration (mg L^{-1})	Final pH	C_e (mg L^{-1})	q_e experimental (mg g^{-1})
0	0	0	0
47.5	9.4	1.70 ± 0.1622	45.32 ± 0.8607
67.6	9.1	3.43 ± 0.0973	63.32 ± 0.8792
97.1	10	6.98 ± 0.2883	88.63 ± 1.053
115.6	10.3	16.33 ± 1.578	97.98 ± 1.145
137.5	10.4	30.45 ± 2.418	106.01 ± 1.345
180.7	10.7	60.56 ± 1.161	120.11 ± 1.161
255	10.8	117.01 ± 6.992	136.16 ± 6.137

Table S7. Isotherm parameters of BPA adsorption on MSN-CTAB.

Langmuir	
Q_{max} (mg g^{-1})	128.19
K_L (L mg^{-1})	0.2829
$R^2_{ajd.}$	0.9746
Reduced Chi-squared	49.526
Freundlich	
K_F (mg g^{-1} (mg $L^{-1})^{-1/n_F}$)	51.159
n_F	4.7451
$R^2_{ajd.}$	0.9716
Reduced Chi-squared	55.489
Liu	
Q_{max} (mg g^{-1})	**155.78**
K_g (L mg^{-1})	0.1567
n_L	0.5873
$R^2_{ajd.}$	**0.9851**
Reduced Chi-squared	29.045

Q_{max}: maximum amount adsorbed; K_L: Langmuir equilibrium constant; $R^2_{adj.}$: adjusted coefficient of determination; K_F: Freundlich equilibrium constant; n_F: dimensionless exponent of the Freundlich equation; K_g: Liu equilibrium constant; n_L: dimensionless exponent of the Liu equation.

References

1 S. Lagergren, *K. Sven. Vetensk. Handl.* , 1898, **24**, 1-39.

2 Y. S. Ho and G. McKay, *Chem. Eng. J.*, 1998, **70**, 115-124.

3 G. Blanchard, M. Maunaye and G. Martin, *Water Res.*, 1984, **18**, 1501-1507.

4 Y.-S. Ho, Doctorates > Ph.D., University of Birmingham, 1995.

5 Y. S. Ho, D. A. J. Wase and C. F. Forster, *Environ. Technol.*, 1996, **17**, 71-77.

6 Y.-S. Ho, *J. Hazard. Mater.*, 2006, **136**, 681-689.

7 Y.-S. Ho, *Environ. Sci. Pollut. Res.*, 2014, **21**, 7234-7235.

8 É. C. Lima, M. A. Adebayo and F. M. Machado, in *Carbon Nanomaterials as Adsorbents for Environmental and Biological Applications*, eds. C. P. Bergmann and F. M. Machado, Springer International Publishing, 1 edn., 2015, DOI: 10.1007/978-3-319-18875-1, ch. 3, pp. 33-69.

9 A. A. Inyinbor, F. A. Adekola and G. A. Olatunji, *Water Resour. Ind.*, 2016, **15**, 14-27.

10 I. Langmuir, *J. Am. Chem. Soc.*, 1918, **40**, 1361-1403.

11 H. M. F. Freundlich, *J. Phys. Chem.*, 1906, **57**, 385-471.

12 R. J. Alessio, X. Li and D. F. Martin, *J. Environ. Sci. Health A Tox. Hazard Subst. Environ. Eng.*, 2012, **47**, 2198-2204.